Analysis of tool geometry in dissimilar Al alloy friction stir welds using optical microscopy and serial sectioning

H. Izadi*[1], J. Fallu[1], A. Abdel-Gwad[2], T. Liyanage[3] and A. P. Gerlich[4]

The influence of tool geometry on material flow during friction stir welding of dissimilar aluminium alloys is investigated. Sheets of Al 2024 and Al 6061 alloys are friction stir welded in lap and butt configurations using different welding conditions. Optical microscopy with serial sectioning is utilised to systematically study material flow when small variations are made to the tool pin. It is shown that three flat features on the pin impose vertical material flow which can promote intermixing. When a threaded tool is used, the material flow and formation of the intermixed region depends on the orientation of the base materials, since the differences in viscosity of material on the advancing versus retreating side of the tool will inhibit intermixing. Decreasing the travel speed will promote intermixing by increasing the residence time to compensate for the differences in material viscosity that otherwise limit intermixing.

Keywords: Friction stir welding, Dissimilar welding, Aluminium, Tool geometry, Material flow, Al 6061, Al 2024

Introduction

Since its development by the Welding Institute in 1991, friction stir welding (FSW) has become an established method for joining aluminium alloys,[1] and a tremendous amount of welding research has been focused on this process.[2,3] The material flow during FSW is a critical feature which determines the formation of defect free joints and the microstructural features within the weld. In particular, the influence of tool geometry and processing parameters is rather complex and closely coupled with many interactions. Consequently, studying the material flow has been approached by many different techniques in recent years, using various techniques such as tracking of tracer particle post-welding by microscopy,[4,5] microstructural analysis of dissimilar alloy joints,[6,7] *in situ* observation using X-ray transmission systems,[8] simulation by numerical modelling[9–12] and using analogue materials like coloured plasticine.[13] Using these techniques, various details may be inferred from analysis of the output.

Many assumptions have been made regarding the role of different tool geometry features; however several characteristics that were traditionally assumed have finally been confirmed experimentally. For example, a combination of material flow numerical modelling followed by validation using tracer particles has shown that the peculiar movement of material ahead of the rotating tool was found to take a semicircular path, and arrive at nearly the same axial position on the trailing side of the tool.[12] The movements of material downwards by the threaded features on the pin have also been confirmed using a combination of modelling and tracer particle validation.[14] Other insights have been gained from numerical modelling, where localised pressure concentrations were observed when flat sections are added to a circular pin.[15] This localised pressure gradient likely accounts for grain refinement observed when these flat features are added to the pin surface compared to cylindrical or threaded profile.[16]

Although a number of studies have applied dissimilar welding to reveal the role of geometry on the material flow, a systematic comparison of similar tools with small variations in one or two geometric features is not available, aside from some comparisons between smooth versus threaded tool pins.[14,17] Another method which can provide valuable insights into determining the material flow during FSW is the use of optical microscopy combined with serial sectioning. This provides the ability to spatially resolve features in all three dimensions when dissimilar alloys are welded; however, it has been seldom applied to friction stir welded structures as it is particularly time consuming.[18] The present work systematically compares the material flow produced by three different tool pin geometries when examining dissimilar lap welds between 6061 and 2024 aluminium alloys, as well as butt welds using serial sectioning. The objective is to discriminate between the role of threads and flats in terms of material flow as compared to a simpler tool with only grooves.

[1]Department of Chemical and Materials Engineering, University of Alberta, Edmonton, Alta T6G 2V4, Canada
[2]Mining and Metallurgical Department, Faculty of Engineering, Al-Azhar University, Qena, Egypt
[3]Hitachi Power Systems Canada Ltd, 826 58th Street East, Saskatoon, Sask. S7K 5Z4, Canada
[4]Department of Mechanical and Mechatronics Engineering, University of Waterloo, Waterloo, Ont. N2L 3G1, Canada

*Corresponding author, email hizadi@ualberta.ca

Published by Maney on behalf of the Institute
Received 5 December 2012; accepted 16 January 2013
DOI 10.1179/1362171813Y.0000000107

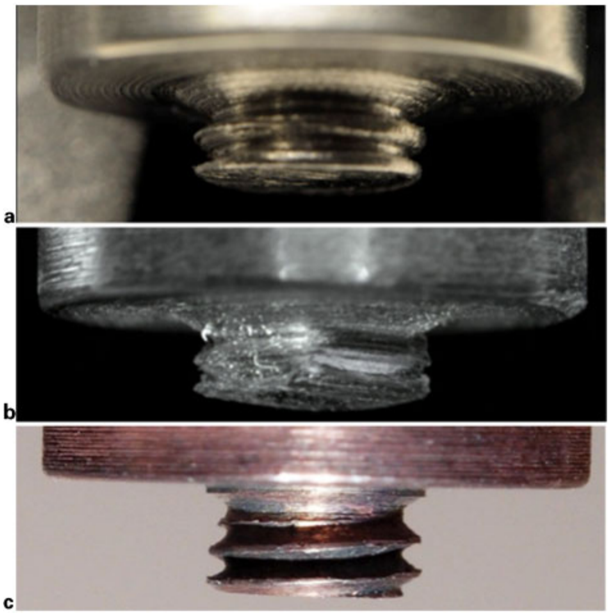

a grooves with 0·7 mm spacing without helix; *b* grooves with 0·7 mm spacing without helix plus three flats on sides of pin every 120°; *c* conventional threaded pin with M4 screw profile (0·7 mm thread spacing with helix)

1 Tool geometries studied, each consisting of 10 mm diameter shoulder and 4 mm diameter pin with different pin profiles

Experimental

The tools employed during FSW had identical shoulder and pin diameters of 10 and 4 mm respectively; however, three slightly different pin geometries were considered as shown in Fig. 1. The tools are designated as follows: grooved pin, which has two concentric ridges; three flat pin, which has the same concentric ridges as the first tool, but three 0·5 mm deep flat spots at every 120° around the pin; and threaded pin, which has a conventional spiral thread following a standard M4 metric screw profile. This provided a direct comparison between the role of flat features (grooved versus three flat), and the role of a helical orientation to the side grooves (grooved versus threaded). The tools were all fabricated from H13 die steel and heat treated to 46–48 HRC.

Friction stir welding of dissimilar alloys Al 2024-T351 and Al 6061-T6 was conducted in both the lap weld and butt weld configurations (Fig. 2). The Al 2024 alloy had a nominal chemistry of Al–4·5Cu–1·4Mg–0·5Mn, and the Al 6061 had a nominal chemistry of Al–1·0Mg–0·6Si–0·25Cu with <0·7Fe and <0·35Cr, Zn, all in wt-%. The tool rotation speed was maintained at 894 rev min^{-1}, and both clockwise and counterclockwise directions were investigated while the travel speed was 88 mm min^{-1} during lap welding, and 33–88 mm min^{-1} during butt welding. Lap welding was conducted with the Al 6061 material which was rolled to a 1 mm thickness and placed on top of the Al 2024 alloy plate.

Optical microscopy was conducted using standard metallographic techniques, with final polishing done using 1 μm diamond suspension, followed by etching with Keller's reagent. Transverse sections of the lap and butt welds were examined, and serial sectioning of the butt welds made using the threaded tool was conducted by grinding and polishing the horizontal (plan view) sections where the tool was frozen in the joint by switching off the machine power. An optical micrograph was generated at depth intervals of 60 μm from the top of the sheet down to the bottom of the pin. Strong contrast was obtained between the two alloys following etching, and the images were processed according to binary colour based on this contrast using Photoshop, where the dark regions correspond to Al 2024 alloy, and the Al 6061 alloy is set as a transparent layer. The horizontal layers were then aligned and assembled into three-dimensional structures for visualisation.

Results and discussion

Grooved pin tool

During dissimilar lap welding, the grooved pin tool produced negligible intermixing between the upper and lower sheets (*see* Fig. 3). Since the Al 2024 alloy on the bottom of the welded was etched preferentially, it is clearly evident that the interface between the two materials is nearly undisturbed. The sheets could easily be pried apart following welding, indicating that only superficial bonding occurred in lap weld shown in Fig. 3, with negligible metallurgical bonding between the sheets. The horizontal alignment of the grooves on this pin geometry does not promote vertical intermixing between the alloys, and only some lamellar flow patterns are evident in the 2024 sheet material stir zone. In prior work, it was found that the formation of bands and lamellae in the stir zone was typically attributed to flow produced by threaded tools;[19] however, more recent work has shown that these microstructural features may also occur with a smooth cylindrical pin when variations in second phase particle distribution or grain sizes occur.[20]

When dissimilar butt welding was conducted using the grooved pin tool, a wavy boundary between the two materials was formed. This wavy boundary occurred regardless of whether the Al 2024 or the Al 6061 alloy

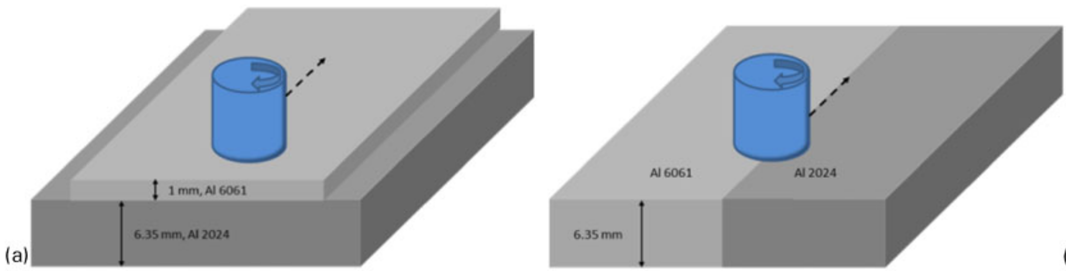

2 Joint configurations considered: *a* lap welding and *b* butt welding shown with Al 6061 on advancing side

3 Lap weld produced using groove tool at 88 mm min^{-1}

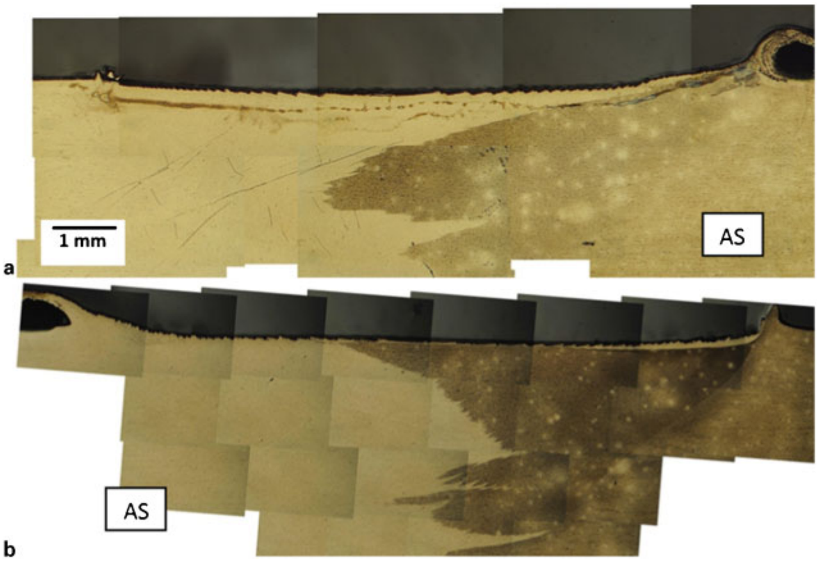

4 Butt welds produced using travel speed of 33 mm min^{-1}, with *a* 2024 and *b* 6061 on advancing side

material was located on the advancing side, and optical micrographs depicting both cases are shown in Fig. 4. It is interesting to note that an onion ring stir zone structure does not form;[21] however, similar wavy interfaces were also produced during dissimilar butt welding of Al 2024 and Al 7075 alloy sheet materials when very low tool rotation speeds of 400 rev min^{-1} are used.[22] Despite the use of higher rotation speeds in the present work (894 rev min^{-1}), no intermixing could be promoted using the grooved pin tool geometry.

Three flat tool

When flat spots are present on the sides of the tool pin, these induce a recirculating flow which entrains material from the upper sheet downwards during lap welding, and leads to the formation of onion ring-like structures which were not observed when using the simple groove tool without flats.[21] The presence of intermixed lamellae containing alternating layers of Al 2024 and Al 6061 is shown in Fig. 5, indicating that the Al 6061 material from the upper sheet moved downwards into the Al 2024 lower sheet. The chemistry of some of these lamellae was confirmed using SEM and energy dispersive X-ray spectroscopy (EDX) analysis shown in Fig. 6, in which the darker etching regions containing Al 2024 alloy were also found to be rich in Cu, as shown in the EDX map in Fig. 6*b*. One of the striking features of the onion ring features formed by the intercalated alloy layers is that there is an inflection in the formation of the lamellae, and they are not arranged in elliptically shaped continuous arcs as typically observed.[19,20] This inflection is most evident near the central region of the stir zone and its profile is highlighted by the labels in Fig. 5.

The observation that flat spots promote vertical intermixing along the length of the pin is analogous to the use of impeller agitators or baffles in chemical reactor design. The formation of a so called double loop recirculating flow is a characteristic feature of radial

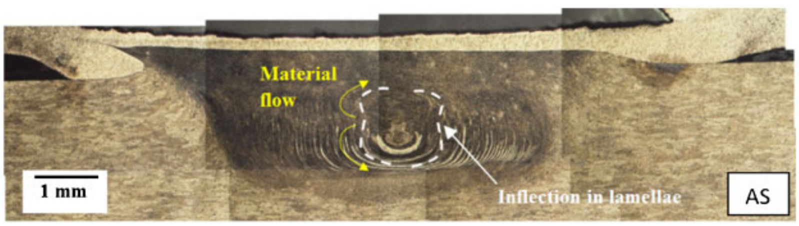

5 Lap weld produced using groove tool with three flats and travel speed of 88 mm min^{-1}

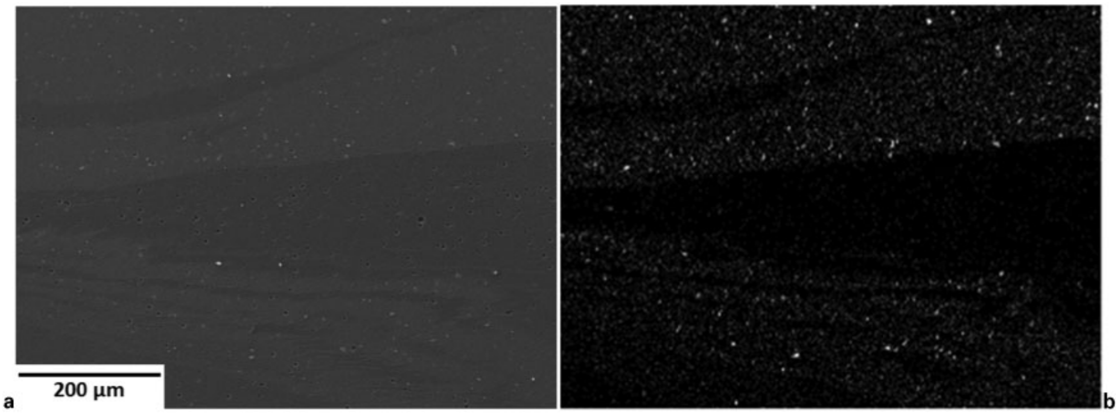

6 Image (SEM) of intermixed region in dissimilar alloy weld showing *a* secondary electron image and *b* EDX mapping of copper

flow impeller design,[23] and this flow pattern can be easily shown using both numerical modelling and particle image velocimetry.[24] The double loop flow which carries material both upwards and downwards (as indicated by the arrows in Fig. 5) is driven by the high pressure region at middle of the impeller, or in this case, the flat region of the tool pin. This high pressure region has already been shown to form on the flat features of FSW pin tools.[15]

It is argued that the presence of flat spots on the tool will function as impeller features within the stir zone, and the flow produced when these flat spots are aligned parallel to the axis of rotation will lead to the formation of the so called double loop recirculating vertical flows upwards and downwards as indicated by the yellow arrows in Fig. 5, with the flow emanating from near the midpoint of the pin. It should be noted that this vertical flow has occurred without the aid of threaded or screw-like features, and this has been widely demonstrated when simple flat panels are used to promote mixing.[25] The double loop flow has led to the formation of an inflection labelled in Fig. 5, and this occurs where the high pressure flow region would originate in the presence of agitator driven flow in a mixing vessel. This vertical recirculating flow has promoted the incorporation and intermixing of the upper Al 6061 into the stir zone.

When the Al 6061 material incorporated into the stir zone in Fig. 5 is intermixed by a recirculating flow, it is expected that one intermingled layer of each alloy or lamella would be formed during each rotation of the tool. To determine the feasibility of intermixing occurring on each rotation via this recirculating flow, the number of tool rotations in the stir zone width area was compared to the number of lamellae. Since the measured width of the stir zone was $\sim 5{\cdot}7$ mm, at a linear travel speed of $1{\cdot}47$ mm s^{-1} the material in the intermixed region will endure a residence time in the stir zone of $\sim 3{\cdot}9$ s. At a rotation speed of 894 rev min^{-1} (or $14{\cdot}9$ rotations per second), there are expected to be 58 individual lamellae in the onion ring pattern of the stir zone intersected from the centre to the boundary of the stir zone. In comparison, there were 49 lamellae observed in Fig. 5; however, the thickness of the lamellae progressively decreased towards the outer boundary of the stir zone, making them difficult to distinguish as distinct layers. However, this does support the notion that each layer was formed during one rotation and an agitator intermixing effect[25] is induced by the flat regions on the pin.

The formation of intermixed lamellae was also promoted by the presence by the flat features on the tool pin during butt welding (*see* Fig. 7*a*); however, these only formed when the Al 2024 alloy was located on the advancing side of the weld (*see* Fig. 7*a*). In both cases in Fig. 7, the upper half of the weld zone mainly contained the material located on the retreating side, due to the large shearing force induced by the tool shoulder. When the Al 2024 is on the advancing side, intermixing occurs between the two alloys (*see* Fig. 7*a*), and a discontinuity in the flow is formed near the location where an inflection occurred in the flow during lap welding (*see* Fig. 5).

When the Al 6061 alloy was located on the advancing side (*see* Fig. 7*b*), there are two lobes produced in the stir zone indicated by the arrows; however, there is no indication of intermixing or onion ring structures. A similar observation was made when dissimilar FSW was studied between Al 6082 and Al 2024 alloys, where intermixing did not occur if the Al 2024 was on the advancing side of the butt weld.[26] The centre of these two lobes is located at locations below the surface of the weld which would correspond to the crest or peak edge of the groove features on the tool (*see* Fig. 1*a*). These lobes likely promoted the enhanced movement of the Al 6061 material into the Al 2024 plate due to the increased tangential velocity produced along the outer surface of these ridges. Based on high temperature tensile strength properties, the Al 6061 alloy exhibits a higher tensile stress than Al 2024 alloy in the temperature range $>300^{\circ}C$,[27] and when the tool rotation is oriented with the Al 6061 alloy on the advancing side, it will be more reluctant to produce in the intermingled or onion ring structures when it is swept into the Al 2024 side ahead of the tool. An analogous scenario occurs when two viscous polymers are sheared together during laminar flow, where the thickness of lamella produced is proportional to the viscosity of the corresponding layers.[28] This explains the thick lobes of Al 6061 which are displaced into the Al 2024 material in Fig. 7*b*.

Helical thread tool

The conventional approach to FSW involves a simple threaded tool with a standard right hand thread (as shown in Fig. 1*c*) which is rotated counterclockwise such that the surface angle of the helical threads

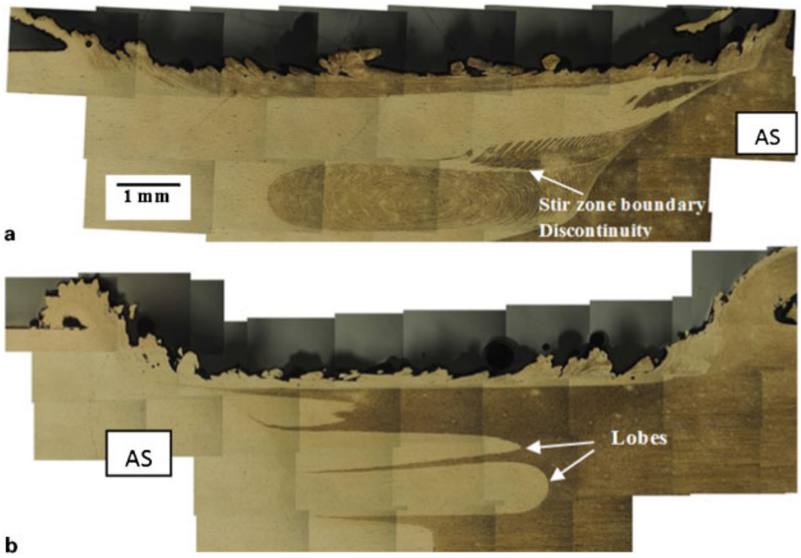

7 Butt welds produced using groove tool with three flats with *a* 2024 on advancing side and *b* 6061 on advancing side

promotes the auger-like movement towards the end of the tool pin. Normally, this flow direction is established during friction stir seam welding, and there is a resulting transfer of material in the opposite direction on the outer boundary of the stir zone which brings material back towards the tool shoulder, and produces recirculating flow.[29,30] When this counterclockwise tool rotation was applied during lap welding, the movement of the upper Al 6061 sheet downwards was also observed as shown in Fig. 8*a*. The lobe of Al 6061 material at the centre of the weld extends nearly 1 mm into the lower Al 2024 plate surface, and metallurgical bonding was observed across the sheet interface (compared to Fig. 3 where no bonding occurred using a grooved pin tool). However, the formation of intermixed lamellae and an onion ring structure did not occur. Again, since the Al 6061 alloy has a higher flow stress than Al 2024 alloy $>300^\circ$C,[27,31] this accounts for the poor transfer of Al 6061 material downwards into the Al 2024 lower plate due to the fact that the Al 6061 material has a higher viscosity and will require more time for movement downwards and establish a recirculation flow.

In contrast, when the tool was rotated clockwise to promote movement of the lower sheet Al 2024 upwards into the top sheet, an onion ring structure was produced as shown in Fig. 8*b*. This indicates that establishing a recirculating flow not only depends on the tool geometry, but also the orientation of materials which are being welded. However, when the tool rotation direction is reversed, the lower viscosity Al 2024 material can flow more readily upwards, and a recirculation flow can be established to form the onion ring structure consisting of alternating lamellae of each alloy.

The formation of an onion ring structure comprising intermixed lamellae of material has previously been studied using a combination of numerical modelling and microscopy of dissimilar joints.[30] It was shown that when a threaded tool pin is used, the onion ring structure results from the formation of an inner downward flow near the pin surface, and an upward flow from the bottom to the top of the pin upwards to towards the top sheet during each rotation of the tool. A critical feature of this intermixing mechanism is the transfer of material from the top surface of the sheets to the bottom of the pin via the threads, which is generally believed to suppress the formation of voids or defects within the stir zone. Note that a smooth cylindrical tool produces defect voids more easily when using the same welding conditions compared to a threaded tool.[2]

When the travel speed is increased from 33 to 88 mm $\min^{-1}$ during butt welding, with the threaded tool, the intermixing is limited and the lamella observed in Fig. 7*a* are thicker and incomplete (*see* Fig. 9*a*). These intermingled layers are not continuous, and have a disrupted appearance when the Al 6061 is on the advancing side of the weld. When the Al 2024 is on the advancing side, a wavy profile is produced at travel speeds of 88 mm $\min^{-1}$, with a few short and thick intermixed layers evident on the retreating side, and very fine lamellae in the middle of the stir zone (*see* Fig. 9*b*). A similar wavy stir zone profile is produced during dissimilar welding of Al 2024 and Al 7075 alloys when the travel speed is increased from 40 to 200 mm $\min^{-1}$.[32]

When the travel speed was decreased from 88 to 33 mm $\min^{-1}$ and serial sectioning was used to further investigate the material flow when using the helical thread tool, the formation of intermixed lamellae is more pronounced and occurs regardless of the orientation of the alloys. The key feature of the formation of the intermixed regions, the movement of the downward flow of the material via the pin threads is clearly visible in Fig. 10*a*. In the case of butt welding with Al 2024 on the advancing side, there is a large lobe of material swept across the stir zone and forms a continuous trail of intermixed lamellae as shown in Fig. 10*b*. Animations of the reconstructed serial sections illustrated in Fig. 10 are also available in the supplementary material (Supplementary Material) site for this journal.

Conclusions

A systematic comparison of the influence of geometric features on the FSW tool pin has revealed some interesting features related to stir zone formation and intermixing in dissimilar welds. First, the use of flat spots on the pin surface can promote vertical movement

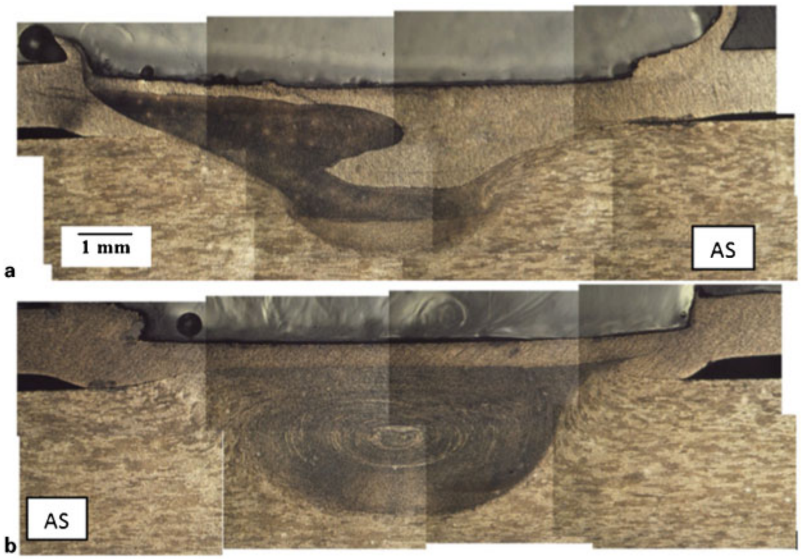

8 Lap weld produced using tool with helical threads on pin when tool rotation is in *a* clockwise (transferring material downwards) and *b* counterclockwise (promoting material movement upwards)

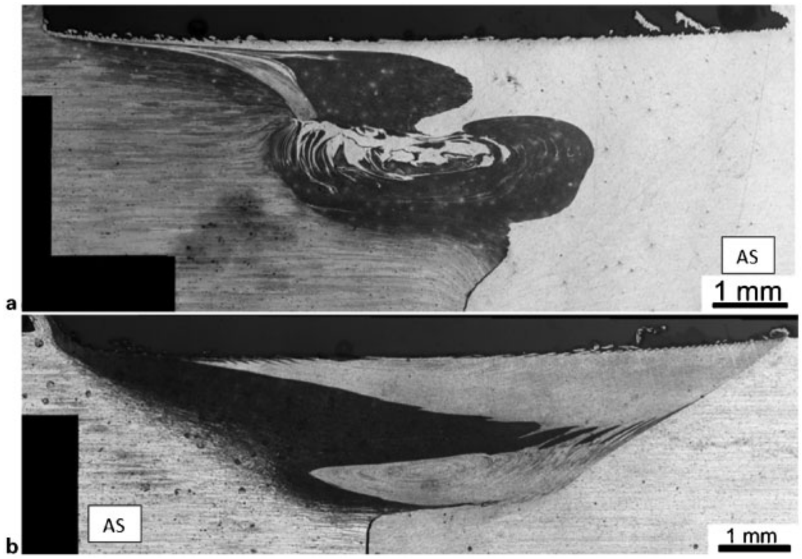

9 Butt welds produced using 88 mm min^{-1} travel speed and spiral tool with *a* 6061 on advancing side and *b* 2024 on advancing side

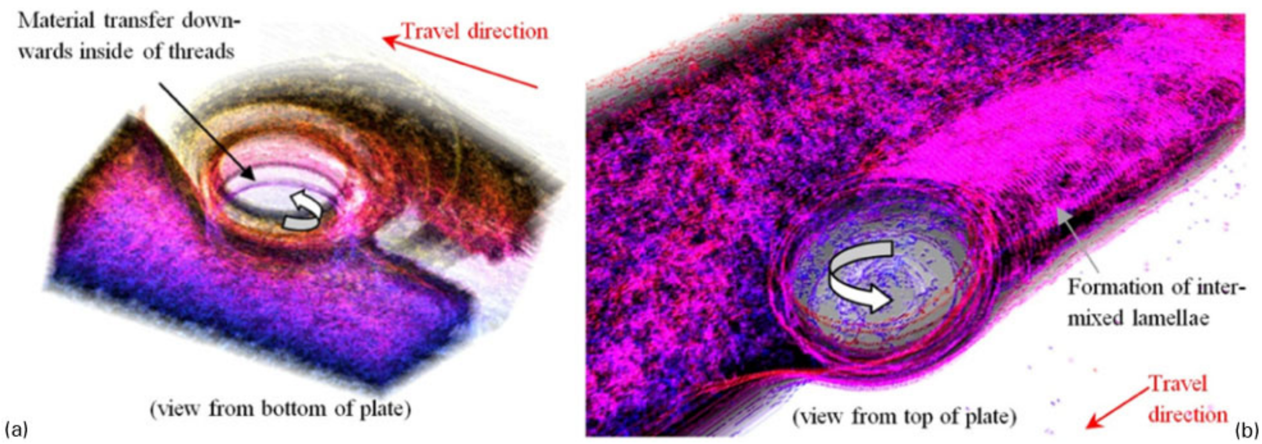

10 Composite images produced from serial sections through the normal plane in butt welds produced using 33 mm min^{-1} travel speed with *a* Al 6061 plate on advancing side and *b* Al 2024 on advancing side

similar to the double loop flow observed in mixing reactors, although this is not as drastic as the flow promoted by helical threads. Second, the use of threaded features is not necessarily a prerequisite for the formation of highly intermixed or onion ring-like structures. Finally, the material flow imposed by the threads is heavily influenced by the position of the base materials. When the tool travel speed is decreased, the intermixing is enhanced by the residence time within the stir zone; however, under certain conditions such as when only grooves (without a helical profile) are used during butt welding or lap welding, or when the Al 2024 alloy is on the advancing side during butt welding, the intermixed lamella are not formed.

Acknowledgements

Financial support for this project was provided by Natural Sciences and Engineering Research Council of Canada (NSERC), and one of the authors (A.A.-G.) acknowledges support from Ministry of Higher Education and Scientific Research of Egypt. The assistance of Matt Dewar with processing of the images is also greatly appreciated.

References

1. W. M. Thomas, E. D. Nicholas, J. D. Needham, M. G. Murch, P. Templesmith and C. J. Daws: 'Friction stir butt welding', GB Patent 9125978·8, 1991.
2. P. L. Threadgilll, A. J. Leonard, H. R. Shercliff and P. J. Withers: 'Friction stir welding of aluminium alloys', *Int. Mater. Rev.*, 2009, **54**, (2), 49–93.
3. R. S. Mishra and Z. Y. Ma: 'Friction stir welding and processing', *Mater. Sci. Eng. R: Reports*, 2005, **50**, (1–2), 1–78.
4. T. U. Seidel and A. P. Reynolds: 'Visualization of the material flow in AA2195 friction-stir welds using a marker insert technique', *Metall. Mater. Trans. A: Phys. Metall. Mater. Sci.*, 2001, **32**, (11), 2879–2884.
5. L. Fratini, G. Buffa, D. Palmeri, J. Hua and R. Shivpuri: 'Material flow in FSW of AA7075-T6 butt joints: Numerical simulations and experimental verifications', *Sci. Technol. Weld. Join.*, 2006, **11**, (4), 412–421.
6. J. H. Ouyang and R. Kovacevic: 'Material flow and microstructure in the friction stir butt welds of the same and dissimilar aluminum alloys', *J. Mater. Eng. Perform.*, 2002, **11**, (1), 51–63.
7. K. U. Kainer: 'Metal matrix composites'; 2006, Weinheim, Wiley-VCH.
8. Y. Morisada, H. Fujii, Y. Kawahito, K. Nakata and M. Tanaka: 'Three-dimensional visualization of material flow during friction stir welding by two pairs of X-ray transmission systems', *Scr. Mater.*, 2011, **65**, (12), 1085–1088.
9. P. A. Colegrove and H. R. Shercliff: 'Experimental and numerical analysis of aluminium alloy 7075-T7351 friction stir welds', *Sci. Technol. Weld. Join.*, 2003, **8**, (5), 360–368.
10. A. Bastier, M. H. Maitournam, K. Dang Van and F. Roger: 'Steady state thermomechanical modelling of friction stir welding', *Sci. Technol. Weld. Join.*, 2006, **11**, (3), 278–288.
11. R. Nandan, G. G. Roy and T. Debroy: 'Numerical simulation of three dimensional heat transfer and plastic flow during friction stir welding', *Metall. Mater. Trans. A: Phys. Metall. Mater. Sci.*, 2006, **37**, (4), 1247–1259.
12. S. Xu, X. Deng, A. P. Reynolds and T. U. Seidel: 'Finite element simulation of material flow in friction stir welding', *Sci. Technol. Weld. Join.*, 2001, **6**, (3), 191–193.
13. B. C. Liechty and B. W. Webb: 'The use of plasticine as an analog to explore material flow in friction stir welding', *J. Mater. Process. Technol.*, 2007, **184**, (1–3), 240–250.
14. P. Su, A. Gerlich, T. H. North and G. J. Bendzsak: 'Material flow during friction stir spot welding', *Sci. Technol. Weld. Join.*, 2006, **11**, (1), 61–71.
15. P. A. Colegrove and H. R. Shercliff: 'CFD modelling of friction stir welding of thick plate 7449 aluminium alloy', *Sci. Technol. Weld. Join.*, 2006, **11**, (4), 429–441.
16. Y. H. Yin, N. Sun, T. H. North and S. S. Hu: 'Microstructures and mechanical properties in dissimilar AZ91/AZ31 spot welds', *Mater. Character.*, 2010, **61**, (10), 1018–1028.
17. P. Su, A. Gerlich, T. North and G. Bendzsak: 'Energy generation and stir zone dimensions in friction stir spot welds', *SAE Tech. Ser.*, 2006, 01–0971.
18. J. A. Schneider and A. C. Nunes Jr: 'Thermo-mechanical processing in friction stir welds', 43–51; 2003, San Diego, CA, TMS (The Minerals, Metals & Materials Society).
19. M. W. Mahoney, C. G. Rhodes, J. G. Flintoff, R. A. Spurling and W. H. Bingel: 'Properties of friction-stir-welded 7075 T651 aluminum', *Metall. Mater. Trans. A: Phys. Metall. Mater. Sci.*, 1998, **29**, (7), 1955–1964.
20. J. H. Yan, M. A. Sutton and A. P. Reynolds: 'Processing and banding in AA2524 and AA2024 friction stir welding', *Sci. Technol. Weld. Join.*, 2007, **12**, (5), 390–401.
21. R. S. Mishra and M. W. Mahoney: 'Friction stir welding and processing'; 2007, Materials Park, OH, ASM International.
22. S. A. Khodir and T. Shibayanagi: 'Microstructure and mechanical properties of friction stir welded dissimilar aluminum joints of AA2024-T3 and AA7075-T6', *Mater. Trans.*, 2007, **48**, (7), 1928–1937.
23. A. W. Nienow: 'Suspension of solid particles in turbine agitated baffled vessels', *Chem. Eng. Sci.*, 1968, **23**, (12), 1453–1459.
24. S. Motamedvaziri and P. M. Armenante: 'Flow regimes and surface air entrainment in partially filled stirred vessels for different fill ratios', *Chem. Eng. Sci.*, 2012, **81**, 231–250.
25. H. A. Jakobsen: 'Chemical reactor modeling: multiphase reactive flows'; 2008, Springer, Berlin.
26. H. R. Shercliff, M. J. Russell, A. Taylor and T. L. Dickerson: 'Microstructural modelling in friction stir welding of 2000 series aluminium alloys', *Mecan. Ind.*, 2005, **6**, (1), 25–35.
27. J. G. Kaufman: 'Properties of aluminum alloys: tensile, creep, and fatigue data at high and low temperatures'; 1999, Materials Park, OH, ASM International.
28. V. W. Uhl: 'Mixing: theory and practice'; 1966, New York, Academic Press.
29. P. Heurtier, M. J. Jones, C. Desrayaud, J. H. Driver, F. Montheillet and D. Allehaux: 'Mechanical and thermal modelling of friction stir welding', *J. Mater. Process. Technol.*, 2006, **171**, (3), 348–357.
30. P. Su, A. Gerlich, T. H. North and G. J. Bendzsak: 'Intermixing in dissimilar friction stir spot welds', *Metall. Mater. Trans. A: Phys. Metall. Mater. Sci.*, 2007, **38**, (3), 584–595.
31. A. M. Handbook: 'ASM metals handbook', Vol. 2, 'Properties and selection: nonferrous alloys and special-purpose materials'; 1992, Materials Park, OH, ASM International.
32. S. A. Khodir and T. Shibayanagi: 'Friction stir welding of dissimilar AA2024 and AA7075 aluminum alloys', *Mater. Sci. Eng. B: Solid-State Mater. Adv. Technol.*, 2008, **148**, (1–3), 82–87.